Discrete-time analysis of cell spacing in ATM systems

F. Hübner[1]
Telecom Australia Research Laboratories, Network Analysis Section, 770 Blackburn Road, Clayton, Victoria 3168, Australia
E-mail: f.huebner@trl.oz.au

P. Tran-Gia
Institute of Computer Science, University of Würzburg, Am Hubland, 97074 Würzburg, Germany
E-mail: trangia@informatik.uni-wuerzburg.d400.de

Received May 1994; revised October 1994

In this paper, an analysis of a general spacer mechanism as used in ATM systems and being part of the usage parameter control functions is developed. The cell process which is subject to spacing can be an arbitrarily chosen renewal process. The algorithm aims at the calculation of the spacer output process in terms of the cell inter-departure time distribution which gives insights to understand the traffic stream forming properties of the spacing mechanism. Two spacer variants are taken into account, where cell rejection and non-rejection versions of the spacing scheme are considered. It is shown that the state process of the *GI/D/1* queue and *GI/D/1* queue with bounded delay can be used to analyze the spacer process. Numerical results are presented to show the system performance for different traffic conditions and system parameters. Beyond the consideration of the pure spacing mechanism, we also take into account that the cell streams are changed between the ATM connection endpoints and the spacer. We model this by considering the output process of a discrete-time *GI/G/1* queue as the spacer input process. We also take the spacer output process as input for a discrete-time *GI/G/1* queue to investigate how the spaced cell stream is again changed until reaching the private/public UNI.

1. Cell spacing mechanism

The design of the user network interface (UNI) in accordance with the incorporated usage parameter control (UPC) function plays an important role in the current ATM development and standardization process. Figure 1 shows a configuration which defines the sequence of reference points and functional groups that the ATM cells

[1] The work for this paper was performed while the author was with the Institute of Computer Science, University of Würzburg, Germany.

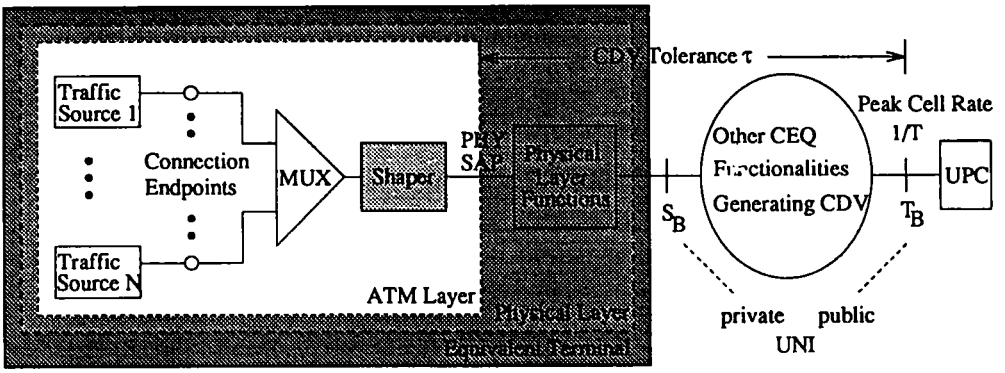

Fig. 1. Reference configuration from ITU-TSS Draft Rec. I.371.

pass on their way from the endpoints of a connection to the UPC. The configuration serves as a reference configuration in the International Telecommunication Union-Telecommunication Standardization Sector (ITU-TSS) [6].

After multiplexing, a traffic shaping function must be performed to avoid that misbehaving traffic sources[2] can deteriorate network performance by generating cells excessively. Leaky-bucket based regulation schemes just as cell spacing have been proposed to perform the traffic shaping function. It should be noted that the leaky-bucket based regulation schemes (contrary to the cell spacing schemes) do not reshape conforming cell streams. At the physical layer service access point (PHY SAP), the peak cell rate of an ATM connection is defined as the inverse of the minimum cell inter-arrival time. Cell delay variation (CDV) is introduced by some physical layer and customer equipment (CEQ) functions between the physical layer service access point (PHY SAP) and the T_B reference point (public UNI). A peak cell rate monitor algorithm that tolerates the CDV (for which the users are not responsible) is proposed by the ITU-TSS [6] and is also adopted by the ATM Forum [1]. Discussions of the dimensioning of the monitor algorithm can be found in [4, 9, 12, 13].

The leaky bucket mechanism has been proposed and investigated as a traffic shaper in several performance studies. In [11], an analytical study has revealed that the usage of a leaky bucket can be very inefficient. Only when the transmission rate that is assigned to a connection is above the leaky bucket permit rate and cells are rejected/marked with a probability greater than 10^{-2}, can the leaky bucket protect the network from misbehaving connections.

The fluid flow approach was used to investigate ON/OFF source traffic and the so-called buffered leaky bucket in [7] and [14]. In [14], two different shaping schemes have been taken into account to incorporate a possibility to give priority

[2] The misbehavior of a source (according to its traffic contract) can be intentionally initiated by the user or can stem from a malfunction of the technical equipment.

to real time over non-real time traffic. In the first scheme, the leaky bucket tokens are accessible for both traffic types and in the second, one dedicated token pool for each of the traffic types is provided. It turned out that the latter scheme provides better flexibility and bandwidth utilization. In [7], the performance of a buffered leaky bucket mechanism and its output process was investigated. An approximation of the output process as coupled Markov Modulated Fluid Sources was proposed and shown to be quite accurate in terms of identical moments of the Markovian approximation and the rate processes.

In the following, we consider cell spacing as a traffic shaping function as it is discussed in recent literature [3–5, 8, 10, 18]. A description of the basic cell spacing functionality is given in section 2.1. The advantage of cell spacing over regulating ATM traffic using a leaky bucket scheme is that cell spacing not only limits the traffic volume, but also reduces its burstiness. This is done at the expense of introducing delay and, therefore, the cell spacing mechanisms must be dimensioned carefully to guarantee the negotiated quality of service (QoS) for each ATM connection.

In [4, 8, 10, 18], architectures and the corresponding traffic models for cell spacers have been proposed. The effects of cell spacing on ATM traffic streams have been discussed in [4, 5, 18] and for a so-called N-level shaper, which constitutes a generalization of the basic cell spacing mechanism in [2]. All performance studies mentioned used either simulation or analytical approaches which are quite limited in terms of not being able to consider realistic ATM traffic scenarios.

In this paper, we derive a very potential analytical approach which allows us to model the ATM traffic which arrives at the shaper (cf. fig. 1) in a very realistic manner. We focus on the change in ATM traffic streams by passing through a cell spacer and derive the cell inter-departure time distribution. Our results are exact if we consider the cell spacer solely and offer a stream of ATM cells which forms a renewal process with general inter-arrival time distribution (see section 2). Then, we take into account that the cell streams are changed between the ATM connection endpoints and the spacer. We propose an approximate solution for the case where cells which are subject to spacing are given by the output process of a discrete-time *GI/G/1* queueing system which models these changes in the cell streams (see section 3). We also propose an approximate solution for the case where the spacer output process serves as an input process for a discrete-time *GI/G/1* queue. By this constellation, we are able to investigate how the spaced traffic streams are changed between the spacer and the private/public UNI. The numerical results are compared with simulation results and it turns out that the approximate results are extremely accurate.

2. Performance analysis

2.1. BASIC MODEL

The relation between the shaper and the spacer is illustrated in fig. 2. Traffic entering the spacer is logically demultiplexed, since each spacer is responsible for

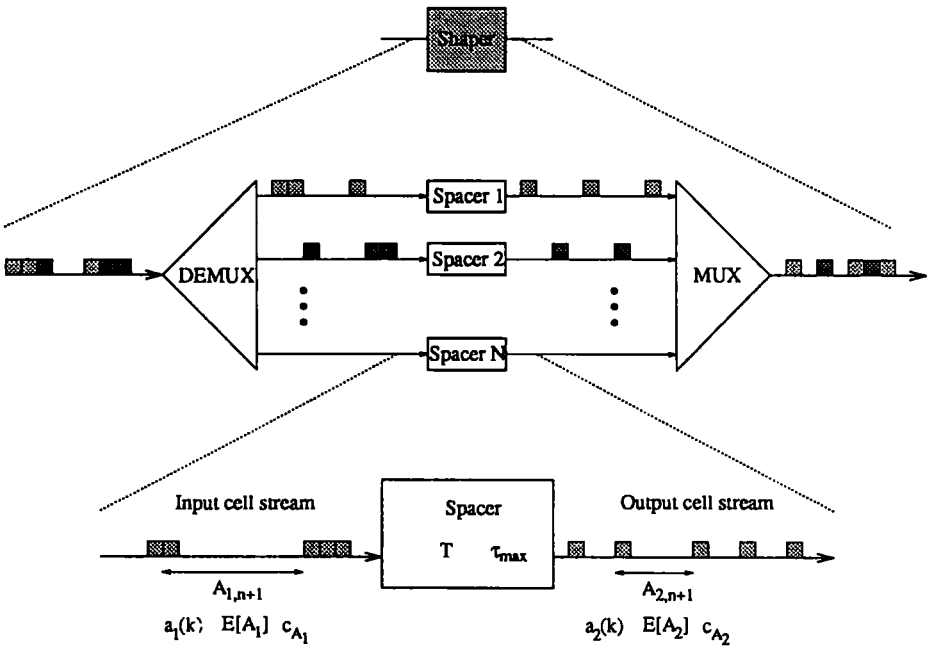

Fig. 2. Basic spacer model.

the cells from exactly one ATM connection. After spacing the different cell streams, they are again multiplexed together. The basic function of a spacer device is to enforce a minimum cell inter-departure time. The bottom part of fig. 2 shows the basic spacer model and the related parameters.

The spacer has to influence the input cell stream in such a way that the time between consecutive cells in the output stream is at least T.[3] This cell stream forming is done by delaying cells which arrive too close together. The time a cell should be delayed is bounded by τ_{max}. Cells which would experience a larger delay are rejected. The purpose is to prevent cells from being delayed too long due to real-time constraints (e.g. according to the negotiated QoS) and to save buffer capacity in the cell spacer.

The time between cells n and $n+1$ is denoted by the random variable (r.v.) $A_{i,n+1}$ ($i = 1$ denoting the input and $i = 2$ the output stream). The corresponding stationary discrete-time distributions and their means and coefficients of variation (CoV) are denoted by $a_i(k)$, $E[A_i]$, and c_{A_i}.

In the next two subsections, we present an exact analysis for the cell inter-departure time distribution $a_2(k)$. In general, the output process is a non-renewal process. The inter-departure time distribution is thus given in conjunction with a

[3] As appropriate for ATM systems, time is discretized into slots of cell duration length. Therefore, we refer to the time interval $x \cdot$ *cell duration* simply as time x.

renewal assumption. The discrete-time inter-arrival time distribution $a_1(k)$ can be chosen as an arbitrary renewal process. In section 2.2, we omit the mechanism of cell rejection, whereas we take it into account in section 2.3.

2.2. ALGORITHM FOR PURE CELL SPACING

If we omit the cell rejection mechanism, the spacer simply delays cells as long as necessary to leave the spacer with inter-cell times of at least T. We present an iterative algorithm to derive the cell inter-departure time distribution of the spacer. The inter-departure time between cell n and $n+1$ is T if cell $n+1$ arrives not later than T after cell n departed from the spacer. Only when a cell arrives more than time T after the preceding cell departed is the cell inter-departure time exactly the inter-arrival time.

The basic idea for the analysis is to introduce a *spacer state* denoted by the r.v. Z_n. Depending on the spacer state Z_n a cell sees upon arrival, the cell has to be delayed a specific amount of time or departs immediately from the spacer. The following notation is used:

Z_n^- r.v. for the spacer state just before the arrival instant of cell n. If Z_n^- is positive, the cell will be delayed by Z_n^- slots, otherwise it will immediately depart from the spacer.

Z_n^+ r.v. for the spacer state immediately after the arrival instant of cell n.

The distributions of the discrete-time r.v.'s Z_n^- and Z_n^+ are denoted by $z_n^-(k)$ and $z_n^+(k)$, respectively. A sample evolution of the r.v.'s Z_n^- and Z_n^+ is shown in fig. 3.[4]

Starting the process in fig. 3 with cell n which needs not be spaced, Z_n^+ is set to T and is then decreased by one in each slot. If cell $n+1$ would arrive within T time slots after the arrival instant of cell n (i.e. Z_n would not be negative), cell $n+1$ would depart T slots after cell n. Since cell $n+1$ arrives later then T time slots after cell n, the inter-departure time $A_{2,n+1}$ is the same as the inter-arrival time $A_{1,n+1}$. Just before the arrival of cell $n+1$, Z_{n+1}^- is negative and therefore Z_{n+1}^+ is set to T. Cell $n+2$ arrives so early that Z_{n+2}^- is positive. Therefore, Z_{n+2}^+ is given by increasing Z_{n+2}^- by T and the departures of cells $n+1$ and $n+2$ are spaced by T. Cell $n+3$ arrives later than T at the spacer but cell $n+2$ is delayed for some slots. According to fig. 3, it happens that cell $n+3$ departs also after T slots. As can be seen, it is possible that under certain circumstances the cell inter-departure intervals are smaller than the cell inter-arrival intervals, although each of the cells has to pass the spacer. This can occur when two consecutive cells are delayed, but the latter cell is delayed less than the former one.

[4] The decrease of the state process values occurs stepwise, since we consider a slotted time axis, but to simplify the illustration we depict it as linear decrease (45° lines).

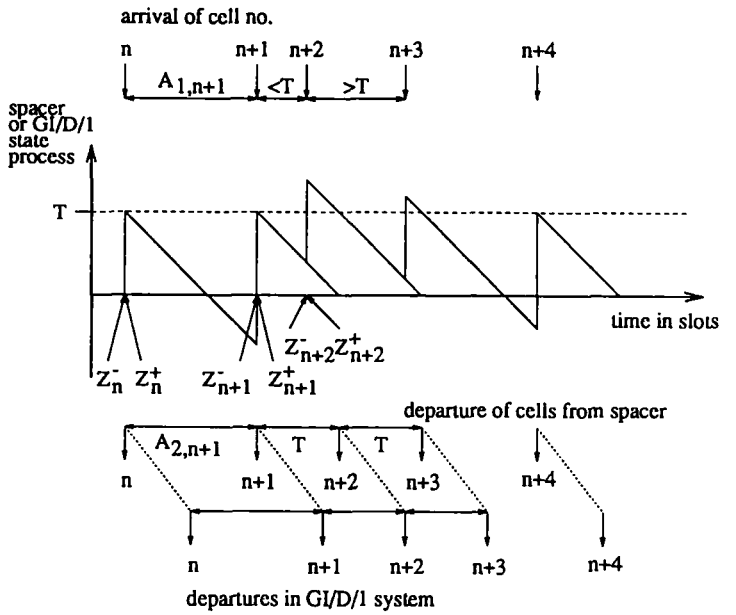

Fig. 3. Snapshot of the spacer state process.

It should be noted here that the state process of the spacer is equivalent to the process of the unfinished work of the *GI/D/1* queue [17]. Thus, the analysis can be used here in an analogous way. The main difference is that the spacer does not have a service period per cell but can deliver cells without sojourn time. The output process of the *GI/D/1* queueing system is shifted by time T compared to the spacer output process (cf. fig. 3).

In the following, we outline an iterative algorithm for the computation of the distributions $z_n^-(k)$ and $z_n^+(k)$, assuming that the cell arrival process constitutes a discrete-time renewal process with general distribution $a_1(k)$. Using the limiting distributions $z^-(k)$ and $z^+(k)$, the cell inter-departure time distribution $a_2(k)$ can be easily derived. We start with the dependencies between the r.v.'s Z_n^- and Z_n^+:

$$Z_{n+1}^- = Z_n^+ - A_{1,n+1}. \tag{1}$$

This equation is driven by the decrease of Z_n by one in each slot. Z_n^+ itself is determined by Z_n^- in the following way:

$$Z_n^+ = \max\{Z_n^-, 0\} + T. \tag{2}$$

According to eq. (2), Z_n^+ is set to T if Z_n^- is negative, otherwise Z_n^+ is given by increasing Z_n^- by T (cf. fig. 3). The related distributions $z_n^-(k)$ and $z_n^+(k)$ can be derived according to eqs. (1) and (2) by

$$z_{n+1}^{-}(k) = z_n^{+}(k) * a_1(-k) \tag{3}$$

and

$$z_n^{+}(k) = \begin{cases} 0, & k < T, \\ \sum_{k'=-\infty}^{0} z_n^{-}(k'), & k = T, \\ z_n^{-}(k-T), & k > T. \end{cases} \tag{4}$$

The "*" operation in eq. (3) denotes the discrete convolution operation. $z_{n+1}^{-}(k)$ is computed using $z_n^{+}(k)$ and $z_n^{+}(k)$ using $z_n^{-}(k)$. Thus, the stationary limiting distributions $z^{-}(k)$ and $z^{+}(k)$ are derived (by iterating eqs. (3) and (4) in an alternating manner) as

$$z^{-}(k) = \lim_{n\to\infty} z_n^{-}(k) \tag{5}$$

and

$$z^{+}(k) = \lim_{n\to\infty} z_n^{+}(k). \tag{6}$$

According to the stability condition for the *GI/D/1* queue, stability is guaranteed for $T/E[A_1] < 1$ (determinsitic service time of T in the *GI/D/1* queue). The probability that a cell is delayed upon its arrival p_d is simply given by

$$p_d = \sum_{k=1}^{\infty} z^{-}(k). \tag{7}$$

By defining the operation $\pi_0(x(k))$ on a distribution $x(k)$ by

$$\pi_0(x(k)) = \begin{cases} 0, & k < 0, \\ \sum_{k'=-\infty}^{0} x(k'), & k = 0, \\ x(k), & k > 0, \end{cases} \tag{8}$$

the distribution for cell delay caused by the spacer can be simply given as

$$P\{\text{spacer delay} = k \text{ slots}\} = \pi_0(z^{-}(k)) \tag{9}$$

As already described above, the time between the departure of the cells n and $n+1$ is T if the value of Z_{n+1}^{-} is not negative. Otherwise, the cell inter-departure time is T plus the number of slots in which the state process was negative until cell $n+1$ arrived. Thus, the cell inter-departure time $A_{2,n+1}$ is given by

$$A_{2,n+1} = \begin{cases} T, & Z_{n+1}^{-} \geq 0, \\ T - Z_{n+1}^{-}, & Z_{n+1}^{-} < 0. \end{cases} \tag{10}$$

The stationary cell inter-departure time distribution $a_2(k)$ can be derived according to eq. (10) as

$$a_2(k) = \begin{cases} 0, & k < T, \\ \sum_{k'=0}^{\infty} z^-(k'), & k = T, \\ z^-(-k+T), & k > T. \end{cases} \tag{11}$$

2.3. ALGORITHM FOR CELL SPACING WITH REJECTION

The spacing mechanism as discussed in the previous subsection can lead to large spacing delay, i.e. the time between the arrival of a cell at the spacer and the departure from it. Thus, a control scheme to guarantee a maximal cell spacing delay can be useful to cope with specific real-time services and their delay constraints. In this subsection, we consider the spacing scheme with rejection. Therefore, we additionally have to incorporate the impact of the delay bound τ_{max} in the analysis. A cell which would be delayed by the spacer more than τ_{max} slots in rejected and has no longer influence on the spacing mechanism. For analysis purposes, we distinguish between the two cases, $\tau_{max} < T$ and $\tau_{max} \geq T$.

The spacer state process is similar to the unfinished work process of a *GI/D/1* queueing system with bounded delay, which was analyzed in [16]. Figure 4 shows a sample path of the spacer state evolution for the case $\tau_{max} < T$. The meaning of Z_n^- and Z_n^+ is the same as in the last subsection (cf. fig. 3).

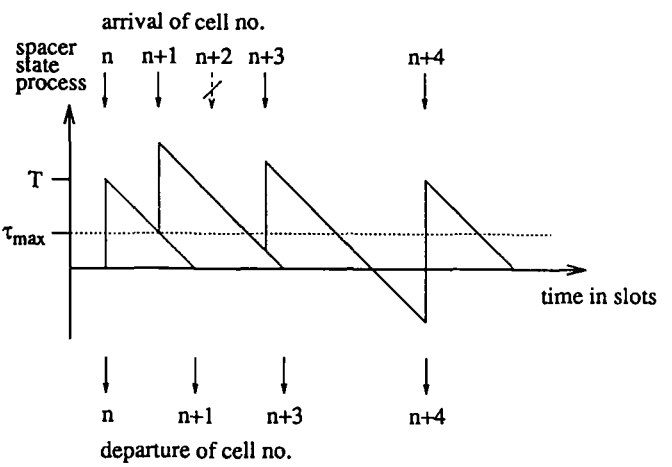

Fig. 4. Spacer state process sample path ($\tau_{max} < T$).

At the arrival instant of cell $n+1$, the r.v. Z_{n+1}^- equals τ_{max} and therefore this cell is not rejected but experiences the maximum delay τ_{max} until departure from the spacer. Since Z_{n+2}^- is larger than τ_{max}, cell $n+2$ is rejected and Z_{n+2}^+ is not increased

compared to Z_{n+2}^-. Z_{n+1}^- depends in the same way on Z_n^+ as described in eq. (1) and the related distribution $z_{n+1}^-(k)$ is given by eq. (3). Z_n^+ is determined by Z_n^- similarly to eq. (2), but the maximum delay τ_{max} must be taken into account:

$$Z_n^+ = \begin{cases} T, & Z_n^- \le 0, \\ Z_n^- + T, & 0 \le Z_n^- \le \tau_{max}, \\ Z_n^-, & Z_n^- > \tau_{max}. \end{cases} \tag{12}$$

This equation is valid for $\tau_{max} < T$ and $\tau_{max} \ge T$, but the related distributions $z_n^+(k)$ are different. For $\tau_{max} < T$, $z_n^+(k)$ is given as

$$z_n^+(k) = \begin{cases} 0, & k \le \tau_{max}, \\ z_n^-(k), & \tau_{max} + 1 \le k \le T - 1, \\ z_n^-(T) + \sum_{k'=-\infty}^{0} z_n^-(k'), & k = T, \\ z_n^-(k) + z_n^-(k - T), & T + 1 \le k \le T + \tau_{max}. \end{cases} \tag{13}$$

Again, $z_{n+1}^-(k)$ can be computed using $z_n^+(k)$ and $z_n^+(k)$ using $z_n^-(k)$. Thus, the stationary limiting distributions $z^-(k)$ and $z^+(k)$ are derived by iterating eqs. (3) and (13). The cell rejection probability p_r is determined by

$$p_r = \sum_{k=\tau_{max}+1}^{\tau_{max}+T} z^-(k). \tag{14}$$

The cell delay distribution introduced by the spacer is given as

$$P\{\text{delay} = k \text{ slots}\} = (1 - p_r)^{-1} \cdot \begin{cases} \sum_{k'=-\infty}^{0} z^-(k'), & k = 0, \\ z^-(k), & 1 \le k \le \tau_{max}. \end{cases} \tag{15}$$

Taking into account the cell rejection probability, the cell inter-departure time $A_{2,n+1}$ is given similarly to eq. (10) by

$$A_{2,n+1} = \begin{cases} T, & 0 \le Z_{n+1}^- \le \tau_{max}, \\ T - Z_{n+1}^-, & Z_{n+1}^- \le 0. \end{cases} \tag{16}$$

Accordingly, the stationary cell inter-departure time distribution $a_2(k)$ is

$$a_2(k) = (1 - p_r)^{-1} \cdot \begin{cases} 0, & k < T, \\ \sum_{k'=0}^{\tau_{max}} z^-(k'), & k = T, \\ z^-(-k + T), & k > T. \end{cases} \tag{17}$$

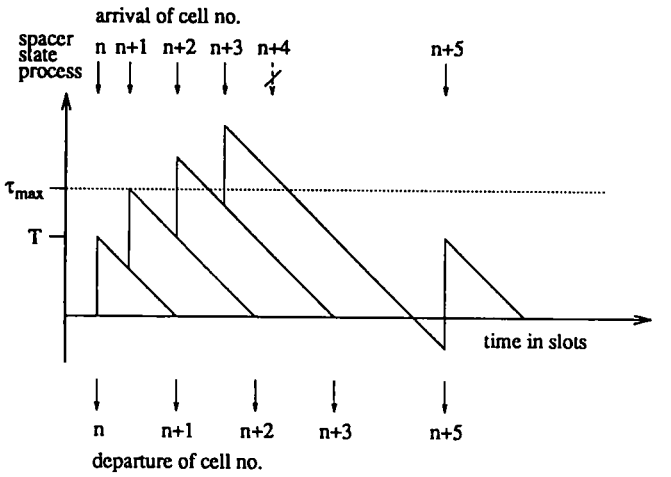

Fig. 5. Spacer state process sample path ($\tau_{max} \geq T$).

A snapshot of the evolution of the spacer state process for $\tau_{max} \geq T$ is depicted in fig. 5.

In constrast to the case $\tau_{max} < T$, several cells can arrive at the spacer close together without being rejected. However, after some time there are too many of them and therefore, for example, cell $n + 4$ is rejected. With the choice of $\tau_{max} \geq T$, it is possible to space bursty input cell streams (e.g. cell arrivals in consecutive slots) without cell rejection. Each of the equations for the iterative algorithm are the same as for $\tau_{max} < T$, except that eq. (13) for $z_n^+(k)$ is altered slightly. For some $\tau_{max} \geq T$, $z_n^+(k)$ is given as

$$z_n^+(k) = \begin{cases} 0, & k < T, \\ \sum_{k'=-\infty}^{0} z_n^-(k'), & k = T, \\ z_n^-(k-T), & T < k \leq \tau_{max}, \\ z_n^-(k) + z_n^-(k-T), & \tau_{max} < k \leq T + \tau_{max}. \end{cases} \tag{18}$$

2.4. NUMERICAL RESULTS

The algorithms derived above allow considerations of arbitrary discrete-time renewal processes as spacer input. To provide systematic parameter studies, in the following we use a negative binomial distribution for $a_1(k)$ to describe the cell arrival process at the spacer:

$$a_1(k) = \binom{k+n-1}{k} p^n (1-p)^k. \tag{19}$$

The mean $E[A_1]$ and CoV c_{A_1} of a negative binomially distributed r.v. A_1 are given according to the parameters p and n by

$$p = (E[A_1]c_{A_1}^2)^{-1} \quad \text{and} \quad n = E[A_1](E[A_1]c_{A_1}^2 - 1)^{-1}. \tag{20}$$

$E[A_1]$ and c_{A_1} can be chosen independently of each other but must fulfill $E[A_1]c_{A_1}^2 > 1$.

In figs. 6–9, we depict some numerical results to show the influences and capabilities of the cell spacing mechanism. Figure 6 shows a specific cell inter-arrival distribution and the corresponding inter-departure time distribution functions for different values of the spacer delay bounds.

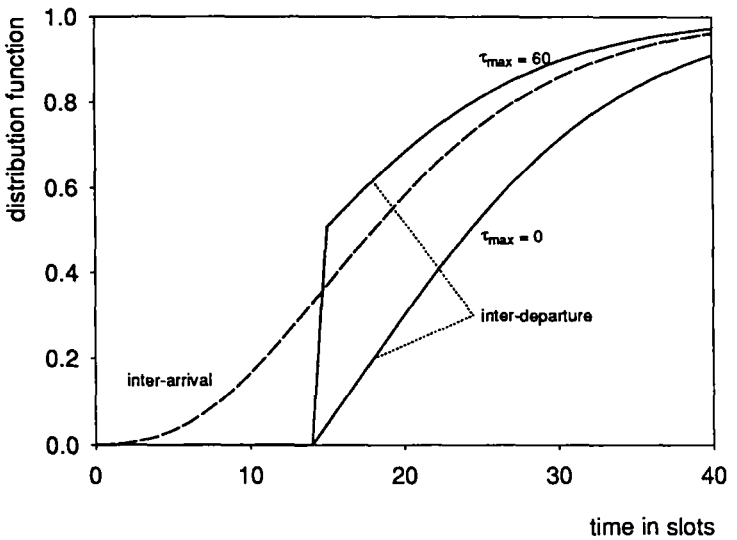

Fig. 6. Comparison of inter-arrival and inter-departure process.

The cell inter-arrival time is negative binomially distributed with mean $E[A_1] = 20$ and CoV $c_{A_1} = 0.5$. The minimum cell inter-departure time from the spacer is chosen at $T = 15$. Accordingly, the inter-departure time distribution function is zero for times smaller than T. Moreover, we can observe a step in the curve for $\tau_{max} = 60$. As shown, due to the spacer function, the inter-departure process can differ considerably from the inter-arrival process.

Table 1 shows some cell delay probabilities p_d (cf. eq. (7)) for the parameter set used in fig. 6 for varying CoV c_{A_1}. It can be observed that more cells are delayed if the CoV increases and this effect demonstrates the capability of cell spacing to form the ATM traffic streams properly.

Table 1

Cell delay probabilities p_d.

c_{A_1}	2.0	1.5	1.0	0.75	0.5	0.25	0.0
p_d	90%	85%	74%	64%	46%	17%	0%

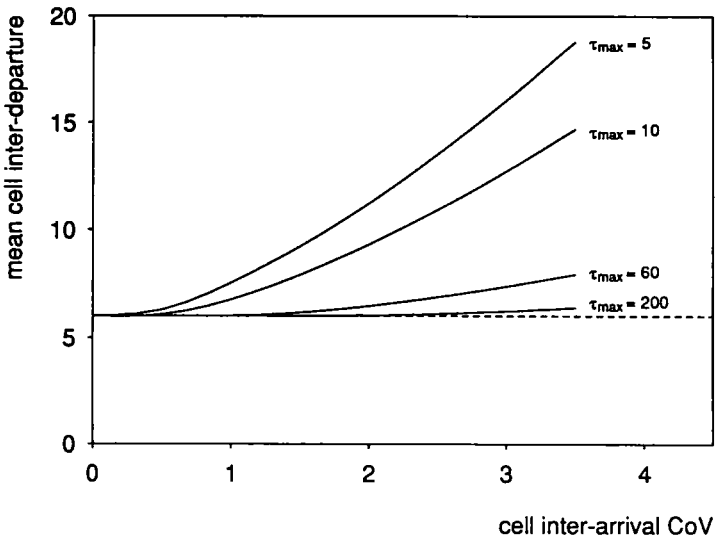

Fig. 7. Influence of spacer delay bound on mean inter-departure time.

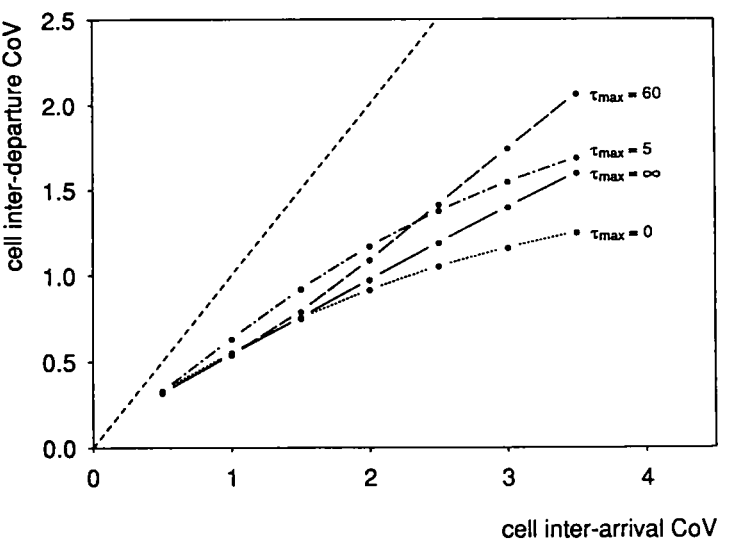

Fig. 8. Process forming capability of cell spacing.

By the employment of the spacer delay bound, cells can be rejected and the inter-departure time distribution (and also its mean) depends strongly on the type of the inter-arrival process and the dimensioning of the maximum spacing delay. This effect is illustrated in fig. 7, where the input process is again described by a negative binomial distribution with mean $E[A_1] = 6$ and minimum inter-departure time $T = 5$. The dotted line indicates the mean cell inter-departure time if no cell spacing would be employed.

The traffic smoothing or variance reduction property of the spacer can be seen in fig. 8, where the CoV of the departure process is plotted as a function of the CoV of the arrival process. The parameters used are the same as for fig. 7. It can be observed that the CoV of the departure process lies below the CoV of the arrival process (we would arrive at the dotted line if no cell spacing would be employed). This effect is intended by the employment of spacing to smooth the cell streams.

By inspecting the curves in fig. 8 more carefully, it can be observed that choosing τ_{max} higher does not necessarily lead to higher CoV in the cell inter-departure process (see e.g. $\tau_{max} = \infty$). The influence of the spacer delay bound on the cell inter-departure process is shown in fig. 9, where the variation reduction property in dependence on the cell delay bound of the spacer is visible.

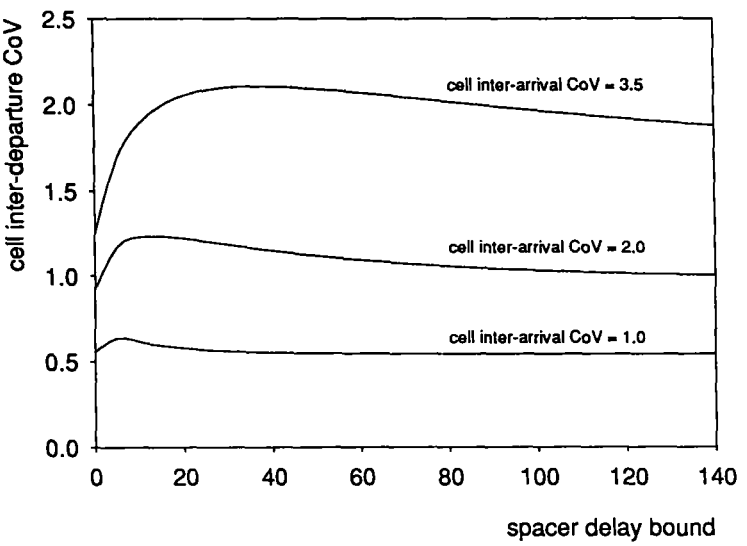

Fig. 9. Influence of delay bound on inter-departure characteristics.

3. Tandem model as overall traffic scenario

In the model presented in the previous section, the input of the spacer was assumed to be a discrete-time renewal process. In this section, we consider the more realistic case that the traffic which is generated by the connection is changed before reaching the spacer and that the spacer output traffic is again changed until reaching the private/public UNI. To model the change in the characteristics of traffic between the ATM connection endpoints, the spacer and the private/public UNI, we adopt a tandem model as depicted in fig. 10.

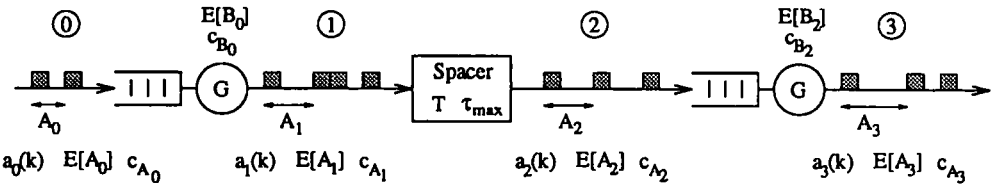

Fig. 10. Tandem model for spacing ATM cell streams.

3.1. CELL PROCESS CHANGES BEFORE SPACER

The change in the characteristics of traffic between the ATM connection endpoints and the spacer output (cf. fig. 1) is investigated by taking the output process of a discrete-time *GI/G/1* queue as the spacer input process (⓪→ ② in fig. 10). The traffic which is generated by a specific ATM connection is described by a discrete-time *GI* distribution and the time between the generation instants of two cells is denoted by the r.v. A_0. The corresponding cell generation distribution is denoted by $a_0(k)$ with mean $E[A_0]$ and coefficient of variation c_{A_0}. The delay introduced between the connection endpoints and the spacer is modeled by the service time of the *GI/G/1* model, which can be arbitrarily chosen. The service time has mean $E[B_0]$ and coefficient of variation c_{B_0}.

In general, the output process of a *GI/G/1* queue is a non-renewal process. To analyze this part of the tandem model, we approximate the *GI/G/1* output process by a renewal process and use this as the input process for the spacer. The output process of the *GI/G/1* queue is evaluated using the algorithm presented in [15].

Since the analytic results for the tandem traffic model as shown in fig. 10 are obtained using a renewal approximation, validations are made by simulations. In fig. 11, the inter-departure time distribution function of the spacer is depicted, where the system configuration is as follows. A *GI/D/1* queue with negative binomially distributed cell inter-generation time ($E[A_0] = 20$, $c_{A_0} = 0.5$ and $c_{A_0} = 2.0$) and deterministic service time $E[B_0] = 4$ delivers a non-renewal output process. This output process is used as the input process for a spacer with parameters $T = 15$ and $\tau_{max} = 5$. The simulation results show that the approximation is extremely accurate, also if quite different cell generation processes ($c_{A_0} = 0.5/c_{A_0} = 2.0$) are used.

The traffic smoothing characteristics of the spacer are depicted in fig. 12, which shows the CoV of the inter-departure process c_{A_2} as a function of the CoV of the inter-arrival process c_{A_0}. Here, the CoV c_{B_0} of the service time in the *GI/G/1* queue is additionally taken into account. The dotted line depicts the case where the input cell stream is neither altered by the *GI/G/1* queue nor by the spacer.

3.2. CELL PROCESS CHANGES AFTER SPACER

The change of the spacer output traffic until reaching the private/public UNI is investigated by taking the output traffic of the spacer as input traffic for the

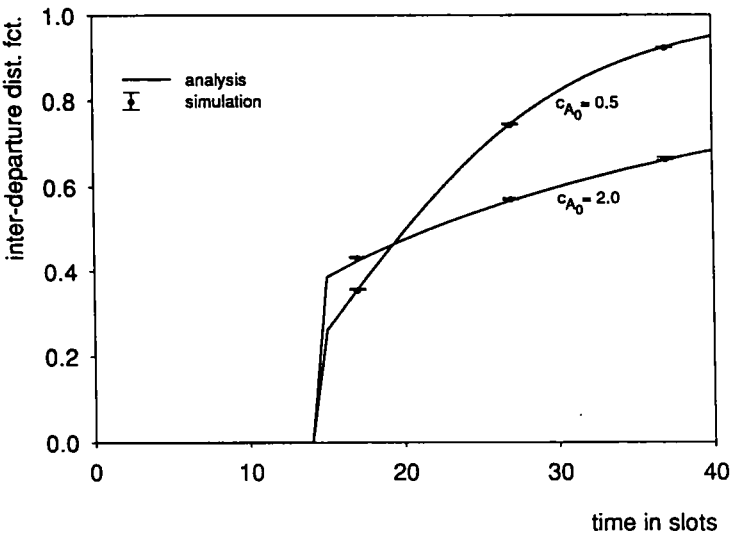

Fig. 11. Approximation accuracy for the tandem model.

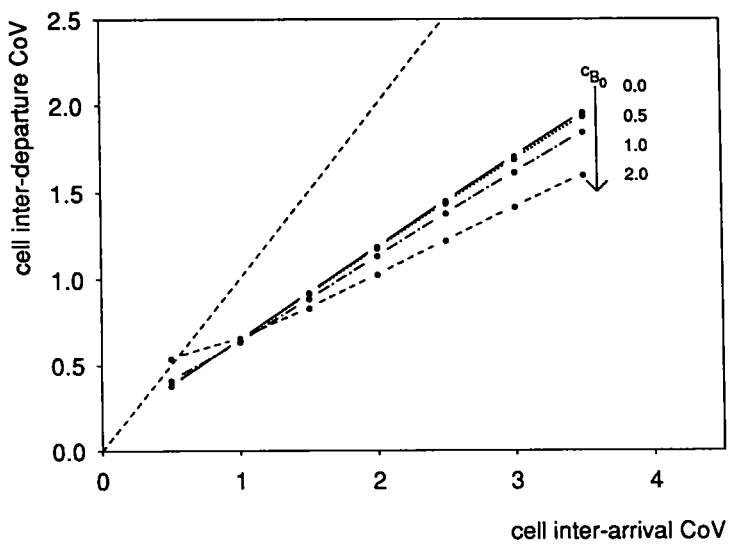

Fig. 12. Smoothing properties in the tandem model.

GI/G/1 queue (① → ③ in fig. 10). The input traffic of the spacer follows a discrete-time *GI* distribution $a_1(k)$. The time between the departures of cells from the spacer is described by the r.v. A_2. The CDV introduced after spacing (between the PHY SAP and the S_B/T_B reference point; cf. fig. 1) is modeled by the service time of the *GI/G/1* queue. The output of the spacer is in general not a renewal process. For analysis

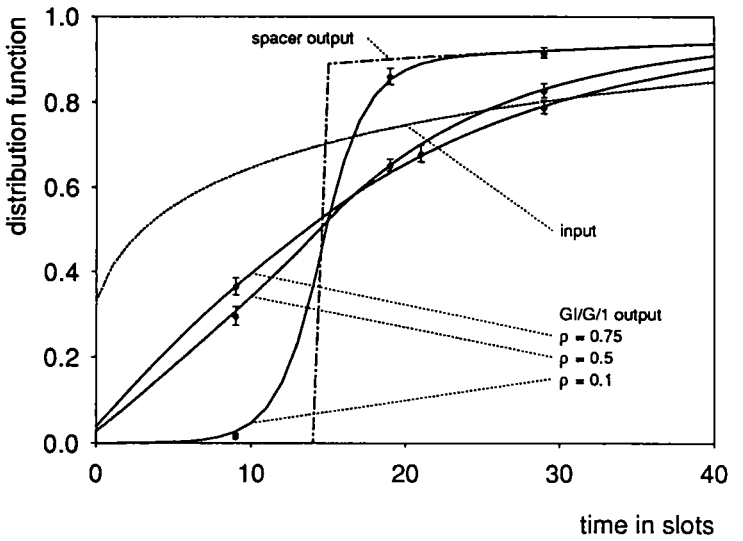

Fig. 13. Change of spacer output process.

purposes, we approximate this output process by a renewal process and take it as the input process for the *GI/G/1* queue.

Figure 13 shows how the spacer input process is changed after spacing (spacer output) by passing through the *GI/G/1* queue (*GI/G/1* output). The input traffic has mean $E[A_1] = 20$ and CoV $c_{A_1} = 2.0$, and the spacer parameters are $T = 15$ and $\tau_{max} = \infty$ (this choice leads to $E[A_2] = E[A_1]$, cf. fig. 7). The service time of the *GI/G/1* queue follows a negative binomial distribution and has mean $E[B_2]$ and coefficient of variation $c_{B_2} = 1.0$. The distribution function of the *GI/G/1* queue output process is depicted for different values of $\rho = E[B_2]/E[A_2]$. It can be observed that the smoothed traffic (spacer output) becomes more bursty after passing through the *GI/G/1* queue. This effect increases with increasing utilization of the resources between the PHY SAP and the private/public UNI (cf. fig. 1), i.e. with larger values for ρ. The renewal approximation again delivers very accurate results, as the simulation results indicate.

4. Concluding remarks

We presented a discrete-time model for cell spacing which performs the shaping function in ATM systems. Algorithms have been developed to calculate the spacer output process distributions. The analysis was carried out in discrete-time domain, based on queueing systems of the types *GI/D/1* and *GI/D/1* with bounded delay. Besides the investigation of the spacing mechanism solely (case (i), where the arrival process at the spacer is an arbitrary renewal process), two submodels have been taken into account: (ii) the arrival process is the output process of a *GI/G/1* queue, and (iii) the spacer process is the input process of a *GI/G/1* queue. The results are given in

terms of the output process distributions, which give insights into the traffic stream forming properties of the spacing mechanism. Two spacer variants have been taken into account, where cell blocking and non-blocking versions of the spacing scheme have been considered. Numerical examples have been presented to show the spacer performance for different traffic conditions and system parameters. The results are exact for the model considered in case (i). For the tandem model (cases (ii) and (iii), an approximation which delivers very accurate numerical results has been presented.

Acknowledgement

The authors would like to thank N. Vicari for valuable programming support.

References

[1] ATM Forum, ATM user-network interface specification, Version 3.0 (1993).
[2] F. Bernabei, L. Gratta, M. Listanti and A. Sarghini, Analysis of ON–OFF source shaping for ATM multiplexing, *INFOCOM 1993*, Paper 11a.3.
[3] P. Boyer, Y. Rouaud and M. Servel, Méthode et système de lissage et de contrôle de débit de communications temporelles asynchrones, French Patent, INPI No. 90/00770 (1990) and European Patent Office Bulletin 91/30 (1991).
[4] P. Boyer, F.M. Guillemin, M.J. Servel and J.-P. Coudreuse, Spacing cells protects and enhances utilization of ATM network links, IEEE Network 6(5) (1992).
[5] F.M. Brochin, A cell spacing device for congestion control in ATM networks, Performance Evaluation 16(1992)107–127.
[6] ITU-TSS Draft Recommendation I.371, Traffic control and congestion control in B-ISDN (1994).
[7] A.I. Elwalid and D. Mitra, Analysis and design of rate-based congestion control of high speed networks, I: Stochastic fluid models, access regulation, Queueing Systems 9(1991)29–64.
[8] F.M. Guillemin, P.E. Boyer and L. Romoeuf, The spacer-controller: Architcture and first assessments, *Workshop on Broadband Communications*, Estoril, Portugal (1992) pp. 313–323.
[9] F.M. Guillemin and W. Monin, Limitation of cell delay variation in ATM networks, *ICCT*, Beijing, China (1992).
[10] F.M. Guillemin and W. Monin, Management of cell delay variation in ATM networks, *GLOBECOM 1992*, pp. 128–132.
[11] M.G. Hluchyj and N. Yin, On the queueing behavior of multiplexed leaky bucket regulated sources, *INFOCOM 1993*, Paper 6a.3.
[12] F. Hübner, Dimensioning of a peak cell rate monitor algorithm using discrete-time analysis, *ITC-14*, Antibes, France, 1994, pp. 1415–1424.
[13] F. Hübner, Output process analysis of the peak cell rate monitor algorithm, University of Würzburg, Institute of Computer Science Research Report Series, Report No. 75 (1994).
[14] L.K. Reiss and L.F. Merakos, Shaping of virtual path traffic for ATM B-ISDN, *INFOCOM 1993*, Paper 2a.4.
[15] P. Tran-Gia, Discrete-time analysis for the interdeparture distribution of *GI/G/1* queues, in: *Teletraffic Analysis and Computer Performance Evaluation*, eds. O.J. Boxma, J.W. Cohen and H.C. Tijms (North-Holland, Amsterdam, 1986) pp. 341–357.
[16] P. Tran-Gia, Analysis of a load-driven overlaod control mechanism in discrete-time domain, *ITC-12*, Turino, Italy, 1988, Paper 4.3a.2.
[17] P. Tran-Gia, Discrete-time analysis technique and application to usage parameter control modelling in ATM systems, *8th Australian Teletraffic Research Seminar*, Melbourne, 1993.
[18] E. Wallmeier and T. Worster, The spacing policer, an algorithm for efficient peak bit rate control in ATM networks, *ISS 14* (1992) Paper A5.5.